Ion **1** reacts with either CO_2 or SO_2 to give a single product ion at m/z 75. We formulate a structure for this product as the 2-silaacetate anion **3**, which can be derived by a metathesis mechanism reminiscent of the Wittig reaction[21] (eq 2). In

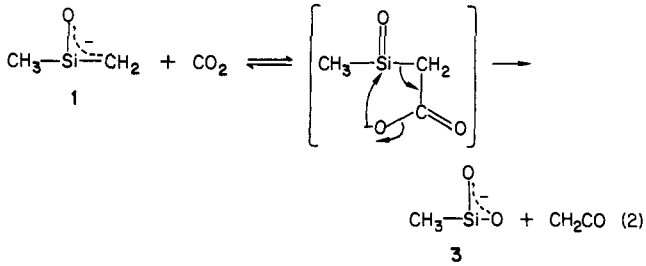

(2)

contrast, acetone enolate undergoes no reaction with either CO_2 or SO_2 under the low-pressure conditions of the FTMS and only slowly associates with CO_2 at higher pressure in a flowing afterglow.[22] As with **1**, $CH_3SiO_2^-$ also fragments by methyl cleavage when collisionally activated, in this case forming SiO_2^- (m/z 60).[23]

Reactions of **1** with a series of Brønsted acids have been examined in order to derive a quantitative measure of its basicity. From the observations summarized in Table I, we assign the proton affinity of **1** to be 366 ± 3 kcal/mol, which is slightly less than the measured value for acetone enolate of 368.8 kcal/mol.[24] This observation is consistent with the relative acidity enhancements noted for other α-silicon acids.[16,25]

Given that this proton affinity estimate is correct, we were surprised to discover that when **1** is allowed to react with either CH_3OD, CH_3CH_2OD, or $(CH_3)_2CHOD$, no H/D exchange occurs in the anion. This is in striking contrast to acetone enolate, which undergoes five rapid H/D exchanges in the presence of each of these reagents.[26] Consideration of the other ionic products from the alcohol reactions listed in Table I suggests a reason for the absence of exchange. Each of the alcohols bearing β-hydrogens yields a product ion at m/z 91 which shifts to m/z 92 in the case of CH_3CH_2OD and $(CH_3)_2CHOD$. Moreover, benzyl alcohol and neopentyl alcohol, which do not possess β-hydrogens, produce only products corresponding to addition with loss of methane. A unified mechanism that accounts for these results is shown in Scheme I. An endothermic proton transfer from alcohol to enolate initially occurs within the energy-rich collision complex (**4** → **5**). With carbon enolates and deuterated alcohols, this is a reversible process which leads to H/D exchange.[27] However, in the present case, the nascent alkoxide is *irreversibly* trapped by the formation of a strong silicon–oxygen bond[28] in adduct **6**. Subsequent decomposition of this intermediate occurs either by methane loss to give the observed silaester enolates (entries j and k, Table I) or by olefin cleavage to produce the silanone hydrate anion at m/z 91. We view this latter process as occurring via a cyclic elimination mechanism (**7** → **8**), similar to ester pyrolysis.[29] The results for the deuterated alcohols offer strong support for this hypothesis. $(CH_3)_2CHOD$ produces the carbon-deuterated silanone hydrate anion (m/z 92) which undergoes a single H/D exchange on oxygen in subsequent encounters with the deuterated alcohol. Furthermore, $(CD_3)_2CDOD$ initially produces only the dideuterated anion (m/z 93), which undergoes no further exchange.

The foregoing results illustrate the rich chemistry of dimethylsilanone enolate. The full details of these experiments as well as additional results for other unsaturated group 4 anions will appear in future publications.

Acknowledgment. B.S.F. acknowledges the National Science Foundation (CHE-8310039) for supporting the advancement of FTMS methodology.

(21) (a) Wittig, G.; Schollkopf, V. *Chem. Ber.* **1954**, *87*, 1318–1330. (b) Johnson, A. W. "Ylid Chemistry"; Academic Press: New York, 1966. (c) Johlman, C. L.; Ijames, C. F.; Wilkins, C. L.; Morton, T. H. *J. Org. Chem.* **1983**, *48*, 2629–2630.

(22) Bierbaum, V. M.; DePuy, C. H.; Shapiro, R. H. *J. Am. Chem. Soc.* **1977**, *99*, 5800–5802.

(23) (a) Nakamura, K.; Hirose, H.; Shibata, A.; Tamura, H. *Jpn. J. Appl. Phys.* **1976**, *15*, 2007–2008. (b) Arnold, F.; Viggiano, A. A.; Ferguson, E. E. *Planet. Space Sci.* **1982**, *30*, 1307–1314. (c) Cooper, D. L.; Wilson, S. *Mol. Phys.* **1981**, *44*, 799–802.

(24) Bartmess, J. E.; McIver, R. T., Jr. In "Gas Phase Ion Chemistry"; Bowers, M. T., Ed.; Academic Press: New York, 1979; Vol. 2, Chapter 11.

(25) Bartmess, J. E., private communication.

(26) DePuy, C. H.; Bierbaum, V. M.; King, G. K.; Shapiro, R. H. *J. Am. Chem. Soc.* **1978**, *100*, 2921–2922.

(27) (a) Stewart, J. H.; Shapiro, R. H.; DePuy, C. H.; Bierbaum, V. M. *J. Am. Chem. Soc.* **1977**, *99*, 7650–7653. (b) Squires, R. R.; Bierbaum, V. M.; Grabowski, J. J.; DePuy, C. H. *J. Am. Chem. Soc.* **1983**, *105*, 5185–5192.

(28) Aylett, B. J. "Organometallic Compounds"; Chapman and Hall: London, 1979; Vol. 1, Part 2.

(29) DePuy, C. H.; King, R. W. *Chem. Rev.* **1960**, *60*, 431–457.

X-ray Absorption Spectroscopy of Nickel in the Hydrogenase from *Desulfovibrio gigas*

Robert A. Scott,*† Sten A. Wallin,† Melvin Czechowski,‡ D. V. DerVartanian,‡ Jean LeGall,‡ Harry D. Peck, Jr.,‡ and Isabel Moura§

School of Chemical Sciences, University of Illinois Urbana, Illinois 61801
Department of Biochemistry, University of Georgia Athens, Georgia 30602
Centro de Quimica Estrutural, Universidades de Lisboa I. St. 1000 Lisbon, Portugal

Received April 5, 1984

Nickel has been identified as an integral component of hydrogenases from a number of different microorganisms, including *Chromatium vinosum*,[1] *Desulfovibrio gigas*,[2] and several *Methanobacterium* species.[3,4] All of these enzymes also contain one or more Fe–S clusters, and the *Methanobacterium thermoautotophicum* enzyme contains a flavin prosthetic group as well. Although the detailed nature of the active sites in these hydrogenases varies among sources, they are all characterized by electron paramagnetic resonance (EPR) signals assignable to a Ni(III) site in some form of the enzyme. There is also evidence for two of the hydrogenases exhibiting magnetic interaction between the Ni(III) site and one or more of the Fe–S clusters. In *D. gigas*, partial reoxidation of the H_2-reduced enzyme generates an EPR signal with $g' = 11.35$ (at X-band)[2] which is reminiscent of the "$g12$" signal observed in some oxidized forms of cytochrome *c* oxidase. In the latter case, this signal has been suggested to arise from coupling of two paramagnetic centers ($Fe_{a_3}^{3+}$ ($S = {}^5/_2$) and Cu_B^{2+} ($S = {}^1/_2$)) resulting in a non-Kramers system.[5]

We have initiated an X-ray absorption spectroscopic (XAS) study of the *Desulfovibrio gigas* enzyme. Our preliminary results reported here indicate that the nickel is reduced from Ni(III) to Ni(II) upon H_2 reduction of the oxidized enzyme and that the ligands are bound to the nickel through sulfur atoms.

The hydrogenase from *Desulfovibrio gigas* (grown on a medium described by LeGall et al.[6]) was purified by ion exchange chromatography as previously described[2] except that the crude extract was obtained by breaking the cells with use of a Gaulin Laboratory Homogenizer rather than with washing. The protein exhibited a single band on disc acrylamide gel electrophoresis.[7] Hyd-

† University of Illinois.
‡ University of Georgia.
§ Universidades de Lisboa.

(1) Albracht, S. P. J.; Kalkman, M. L.; Slater, E. C. *Biochim. Biophys. Acta* **1983**, *724*, 309–316.

(2) LeGall, J.; Ljungdahl, P. O.; Moura, I.; Peck, H. D., Jr.; Xavier, A. V.; Moura, J. J. G.; Teixera, M.; Huynh, B. H.; DerVartanian, D. V. *Biochem. Biophys. Res. Commun.* **1982**, *106*, 610–616.

(3) Graf, E.-G.; Thauer, R. K. *FEBS Lett.* **1981**, *136*, 165–169.

(4) Lancaster, J. R., Jr. *Science* **1982**, *216*, 1324–1325.

(5) Brudvig, G. W.; Stevens, T. H.; Morse, R. H.; Chan, S. I. *Biochemistry* **1981**, *20*, 3912–3921. Hagen, W. R. *Biochim. Biophys. Acta* **1982**, *708*, 82–98.

(6) LeGall, J.; Mazza, G.; Dragoni, N. *Biochim. Biophys. Acta* **1965**, *99*, 385–387.

(7) Brewer, J. M.; Ashworth, R. B. *J. Chem. Educ.* **1969**, *46*, 41–45.

0002-7863/84/1506-6864$01.50/0

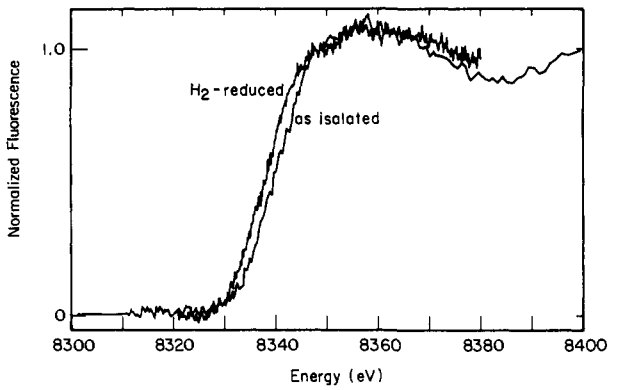

Figure 1. Nickel K-absorption edge spectra for oxidized "as isolated" and H_2-reduced *D. gigas* hydrogenase. The −2-eV shift indicates a decrease in the average nickel oxidation state upon H_2 reduction.

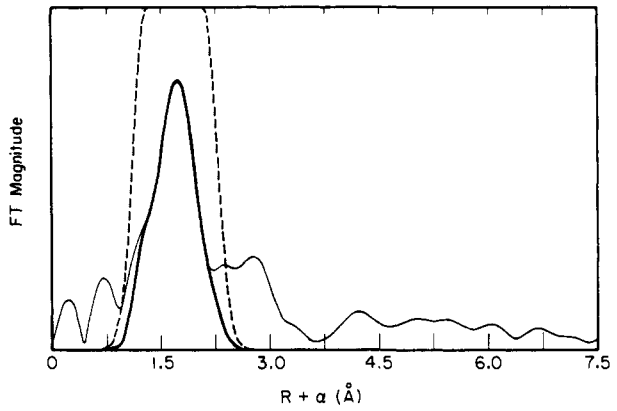

Figure 2. Fourier transform (k = 3.5–10.5 Å^{-1}, k^3 weighting) of Ni EXAFS of oxidized *D. gigas* hydrogenase. The dashed curve represents the filter window used to generate the data in Figure 3. The bold line is the extracted FT peak (i.e., product of window and FT).

rogenase activity was determined by the H_2 evolution assay[8] with H_2 determined by a Varian 4600 gas chromatograph.[2] A typical yield from 4 kg of cells is 800 mg of pure hydrogenase with a specific activity of 400. Plasma emission spectroscopy with a Jarrell-Ash Model 750 Atomcomp was used to determine a nickel content of 0.73 g-atom of nickel per 89 500 g-atom of protein.

The XAS data were collected at the Stanford Synchrotron Radiation Laboratory (SSRL) on the focused beam line II-2 under dedicated conditions (3.0 GeV, ca. 60 mA) with Si[220] monochromator crystals. All protein data were collected by fluorescence excitation with use of scintillation detectors[9] and Co filters. In order to properly analyze the EXAFS data, two model compounds were examined. $[Ni(mnt)_2](n\text{-}Bu_4N)_2$ and $[Ni(mnt)_2](n\text{-}Bu_4N)$ (mnt = maleonitriledithiolate) were prepared by literature procedures.[10] XAS data were collected by standard transmission techniques on SSRL beam line VII-3 under parasitic conditions (1.9 GeV, ca. 15 mA) with Si[220] monochromator crystals. In all cases, internal calibration[11] using a nickel foil standard yielded a 0.2-eV accuracy of the energy scale.

The Ni K-absorption edge spectra of oxidized and H_2-reduced *D. gigas* hydrogenase are shown in Figure 1. The main difference between the two spectra is the ca. 2 eV shift to lower energy of the H_2-reduced edge compared to the oxidized edge. The two model compounds examined consist of Ni(II) and Ni(III) in an essentially square-planar NiS_4 arrangement.[12] The shift observed between the edges of these two compounds is also ca. 2 eV (not shown). Our conclusion is that a substantial fraction of the nickel in the hydrogenase is reduced from Ni(III) to Ni(II) upon H_2 reduction.

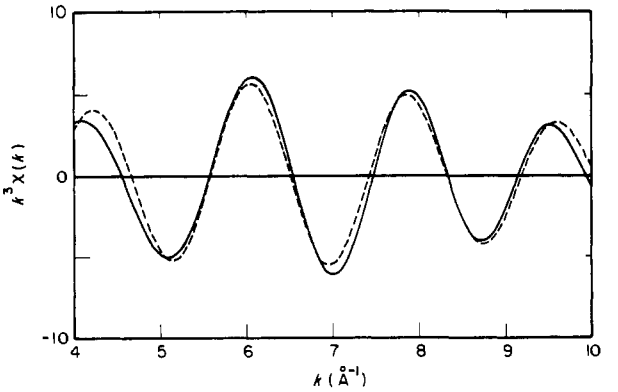

Figure 3. First-shell EXAFS (solid line) extracted as shown in Figure 2 and best fit (dashed line) for oxidized *D. gigas* hydrogenase. The fit corresponds to ca. 4.5 Ni–S interactions with R(Ni–S) = 2.20 Å and $\Delta\sigma^2$ = 0.0052 Å^2 (relative to [Ni(mnt)]$^-$).

The Fourier transform (FT) of the Ni extended X-ray absorption fine structure (EXAFS) data of the oxidized form of *D. gigas* hydrogenase (collected at ca. −60 °C) is shown in Figure 2. The first shell peak was extracted and backtransformed by using a filter window represented by the dashed line in Figure 2. Curve fitting of this filtered data was performed by using phase and amplitude functions derived from complex backtransforms[13] of the nickel model compounds.[14] The resultant fit for oxidized *D. gigas* hydrogenase is compared to the filtered data in Figure 3. Acceptable fits were only obtained by assuming a Ni–S interaction. The best fit Ni–S distance for both oxidized (Figure 3) and H_2-reduced enzyme (not shown) was found to be 2.20 (2) Å. The coordination number calculated from the best fits is ca. 4 for both enzyme derivatives. Although the observed data can be explained by assuming only Ni–S interactions, the presence of a smaller number of low atomic number scatterers in addition to the sulfur atoms cannot be completely ruled out.

A nickel-containing hydrogenase from *Methanobacterium thermoautotrophicum* has recently been examined by XAS.[15] These workers observed Ni–S interactions in the oxidized form of this enzyme as well, raising the possibility that a common nickel active site structure exists in hydrogenases from different sources.

Acknowledgment. J. R. Schwartz and M. Lyons prepared the $[Ni(mnt)_2]^{-,2-}$ compounds. We thank A. V. Xavier and J. J. G. Moura for helpful discussions. This work was supported by a NIH Biomedical Research Support Grant (RR-07030) to R.A.S. and by a National Science Foundation Grant (PCM-8111325) to J.L., D.V.D., and H.D.P. The work was done at SSRL which is supported by the Department of Energy, Office of Basic Energy Sciences, and the NIH, Biotechnology Resource Program, Division of Research Resources.

Registry No. Ni, 7440-02-0; hydrogenase, 9027-05-8.

(8) Peck, H. D., Jr.; Gest, H. *J. Bacteriol.* **1956**, *71*, 248–254.
(9) Cramer, S. P.; Scott, R. A. *Rev. Sci. Instrum.* **1981**, *52*, 395–399.
(10) Davison, A.; Holm, R. H. *Inorg. Synth.* **1967**, *10*, 8–26.
(11) Scott, R. A. In "The Biological Chemistry of Iron"; Dunford, H. B., Dolphin, D. H., Raymond, K. N., Sieker, L. C., Eds.; D. Reidel: Boston, 1982; pp 475–484.
(12) Eisenberg, R. In "Progress in Inorganic Chemistry"; Lippard, S. J., Ed.; Wiley: New York, 1970; Vol. 12, pp 295–369.
(13) Lee, P. A.; Citrin, P. H.; Eisenberger, P.; Kincaid, B. M. *Rev. Mod. Phys.* **1981**, *53*, 769–806.
(14) The curve-fitting approach used the following method for extracting amplitude and phase functions from the model compounds. E_0 was adjusted until the empirical phase function of the model compound EXAFS data (extracted by complex backtransform assuming the known distance) matched the theoretical phase function. With use of this empirical phase function, the known Ni–S distance and coordination number, a fit was performed on the model by using the theoretical amplitude function and by optimizing a scale factor and a Debye–Waller σ. This σ was then used to extract an empirical amplitude function from the model (again, by complex backtransform), and this was used with the empirical phase function to perform fits on the protein data, optimizing distance, coordination number, and σ.
(15) Lindahl, P. A.; Kojima, N.; Hausinger, R. P.; Fox, J. A.; Teo, B. K.; Walsh, C. T.; Orme-Johnson, W. H. *J. Am. Chem. Soc.* **1984**, *106*, 3062–3064.